Full paper / Mémoire

Electrochemical determination of *p*-cresol concentration using zeolite-modified electrodes

David Bergé-Lefranc, Marielle Eyraud*, Oliver Schäf

Laboratoire Chimie Provence, UMR 6264, CNRS − Université de Provence, 13397 Marseille cedex 20, France

Abstract

Carbon paste electrodes modified with different zeolites (MFI and FAU) were studied in order to evidence the electro-oxidation of *p*-cresol. Cyclovoltammetric experiments were applied by direct measurement in *p*-cresol-containing aqueous solution, or during release in solution without *p*-cresol after impregnation. In both cases, the electro-oxidation signal of *p*-cresol led to two oxidation peaks. Different concentrations of *p*-cresol were studied. Influences of charge compensating cations, electrode impregnation time and zeolite type were investigated. It was shown that electrochemical measurements could be used as a detection method for *p*-cresol in aqueous solution with a high sensitivity. ***To cite this article: D. Bergé-Lefranc et al., C. R. Chimie 11 (2008).***
© 2008 Académie des sciences. Published by Elsevier Masson SAS. All rights reserved.

Résumé

Des électrodes à pâte carbone modifiées avec différentes zéolithes (MFI et FAU) ont été étudiées pour mettre en évidence l'électro-oxydation du *p*-crésol, une toxine urémique. Des expériences de cyclo-voltamétrie ont été réalisées directement dans une solution contenant du *p*-crésol ou après imprégnation. Dans les deux cas, deux pics anodiques sont obtenus, correspondant à différents sites d'oxydation (en surface et dans le volume de l'électrode). Différentes concentrations de *p*-crésol ont été utilisées. Les influences des cations de compensation, du temps d'imprégnation de l'électrode et du type de zéolithe ont été étudiées. Nous avons montré que les techniques électrochimiques pouvaient être utilisées comme méthode de détection du *p*-crésol, avec une très grande sensibilité. ***Pour citer cet article : D. Bergé-Lefranc et al., C. R. Chimie 11 (2008).***
© 2008 Académie des sciences. Published by Elsevier Masson SAS. All rights reserved.

Keywords: Zeolite; Uremic toxin; Biosensor; ZME; Cyclovoltammetric

Mots-clés : Zéolithe ; Toxines urémiques ; Biocapteurs ; ZME ; Voltamétrie cyclique

1. Introduction

Renal failure is a syndrome where the kidneys do not fulfill their function of blood epuration leading to accumulation of human metabolism products called uremic toxins. The patient has then to be treated by dialysis during which most of uremic toxins are eliminated, like urea and creatinine. Nevertheless, some of them are not efficiently removed, like protein-bound and high-molecular-weight molecules [1]. Lesaffer et al. [2] found that removal of *p*-cresol is only 29%,

---

versus 75% for urea. This molecule is a small phenolic compound fixed to proteins in healthy conditions. It is produced by the degradation of amino-acids (phenylalanine and tyrosine) due to the activity of intestinal bacteria. This toxin can deteriorate the immunizing defenses by inhibiting the phagocytose capacities of cells like polynuclear neutrophiles [3]. Moreover, it is implied in vascular lesions present in case of renal insufficiency [4]. In order to increase the epuration capacity of dialysis systems, adsorption onto solid materials such as zeolites is explored, because they are supposed to be non-toxic, stable in aqueous solution and have a great joined size selectivity varying with the zeolite used. Wernert et al. [5] have shown that a hydrophobic silicalite MFI zeolite is a good candidate for *p*-cresol adsorption. Currently, *p*-cresol is not part of the toxins that are measured regularly using automatic assays, because the identification of protein-bound solutes in uremic serum is difficult [6]. During this assay, a saline solution coupled with a defecating agent is used in order to isolate *p*-cresol, *p*-cresol being measured by HPLC coupled with a fluorescence module. The liquid phase is a phosphate buffer at 20 mM concentration, passed on a hydrophobic column. The measurement is realized with an excitative length wave of 285 nm and an emission length wave of 310 nm. By this method, the limit of detection is about 1 μM. Nevertheless, this toxin can easily be measured by the UV absorption method [7].

Zeolite-modified electrodes (ZMEs) have generated great interest since the 1980s [8,9] because of a high potential sensitivity. Indeed, zeolites are microporous materials with channel and cage sizes lying between 0.2 and 1.4 nm [10]. They present a large inner surface area. They present high adsorption capacities as molecular sieve and ionic-exchange properties [11]. They can be used for five applications [12]: direct amperometric detection, voltammetric detection after accumulation at open circuit, indirect amperometric detection of non-electroactive species, amperometric biosensors and potentiometric sensors using zeolite membranes. Various ways are reported for the preparation of ZMEs [12], such as covalent binding of zeolite particles to an electrode surface, coating of zeolite embedded in polymeric films on solid electrodes, compression of zeolites on conductive substrates, dispersion of zeolite particles within solid matrices like carbon paste or gold nanoparticles.

Electrochemical detection leads to elaborate biosensors for various bio-molecules in order to obtain healthy and biological information. Researchers have treated during the 2000s a lot of routes and developed various

sensors. In the case of glucose [13], the enzyme was immobilized in the zeolitic structure and amperometric sensors can determine the glucose concentration. Biosensors for NADH cofactor were elaborated using carbon paste doped with zeolite-containing ferrocene [14]. For urea measurement [15], a polymeric membrane sensible to NH_4^+ based on zeolite incorporation was used in addition to the urease enzyme effect. These different zeolite applications consequently allow a specific measurement of one uremic toxin. In the case of *p*-cresol detection, we found only one paper [16] related to a methylphenazonium-zeolite-modified enzyme sensor for the detection of phenols including *p*-cresol, however, not by electro-oxidation. Only few results are available on alcohol electro-oxidation on ZMEs. Among them, Xu et al. [17] indicated the increased activities observed with a carbon paste ZME in comparison with a carbon graphite electrode, in cyclovoltammetric experiments on EtOH and MeOH. Closer to our concerns, the works of Carvalho [18,19] concerning the electro-oxidation of phenol on zeolite/graphite electrodes have also shown a better performance of ZMEs in comparison to Pt electrodes.

The present work focuses on the electrochemical behavior of *p*-cresol in physiological conditions using a carbon paste–zeolite-modified electrode, in comparison with a classical carbon electrode or a simple carbon paste electrode.
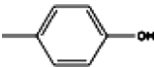
2. Experimental part

2.1. Toxin studied

p-Cresol is also designated as 4-methyl phenol. Its physical and chemical properties are given in Table 1. This molecule has dimensions close to the medium size pores of zeolites (given below). Previous studies reveal MFI type zeolites as good adsorbents for *p*-cresol [20], with an influence of the Si/Al ratio due to the variation of material's hydrophobicity [7]. *p*-Cresol with 99% purity was purchased from Aldrich.

2.2. Zeolites

Zeolite materials are tectosilicates constituted by a succession of interlinked aluminum and silicon tetrahedra. They show void systems of interconnected channels and cavities strictly defined. The presence of trivalent aluminum ions induce a negative charge in the framework to be compensated by extra framework cations. The level of positive charges is therefore directly driven by the quantity of aluminum atoms. The

Table 1
Physical and chemical properties of *p*-cresol

Molecule	Structure	pK_a (298 K)	MW (g mol^{-1})	$C_n{}^a$ (μm)	$C_u{}^a$ (μm)	Sizes (nm)
						x^b
						y
						z
p-Cresol, CH$_3$C$_6$H$_4$OH		10.3	108	7	$>186 \pm 40$	0.43(0.66) 0.64(0.76) 0.18(0.39)

[a] C_n and C_u correspond, respectively, to the normal and the uremic concentrations of *p*-cresol in blood.
[b] Geometric sizes and between round brackets, the sizes determined by Cerius2 software.

MFI type zeolites are constituted by a two-dimensional interconnected channel systems (orthorhombic *Pnma* with $a = 2.01$ nm, $b = 1.99$ nm, $c = 1.34$ nm) [21]. The first channel is straight, with dimensions of 0.56×0.53 nm along the [010] axis, and the other is zig-zag formed with 0.55×0.51 nm dimensions along the [100] axis. The MFI zeolite structure type exists between a pure silica form without aluminum named silicalite and up to Si/Al ratio of 27 with different charge compensating cations named ZSM-5. The MFI material used in this study was purchased from SudChem, the Si/Al ratio is equal to 400 with H$^+$ as the charge compensating cation (referred to as HMFI here).

To evaluate the zeolite composition influence on the alcohol electrochemical oxidation behavior, a sodium form was prepared. For that, parent HMFI was subjected to an ion exchange using an aqueous chloride solution at 1 M concentration at 80 °C for 24 h with a liquid/solid mass ratio equal to 30. The solid was next rinsed with deionized water and dried. It was named NaMFI.

To check the influence of the zeolite structure on the adsorption properties, experiments were performed using FAU-type zeolites. These zeolites are constituted by a tetrahedral three-dimensional channel system with sizes of 0.74×0.74 nm. At interconnections super-cages of 1.24 nm are present. This structure forms a cubic system *Fd*-3*m* with lattice parameters equal to 2.47 nm [22]. FAU used was in H$^+$ form with a Si/Al ratio equal to 80.

The structures and channel systems of the two zeolites employed are summarized in Table 2.

2.3. Characterization methods

SEM/EDX was performed for morphological and chemical composition information (Cambridge S90B with EDAX DX4 SUTV detector).

Specific surface areas were determined by nitrogen adsorption at 77 K with a Micrometrics ASAP 2010 apparatus. Before adsorption, samples were outgassed for 12 h at 150 °C at a pressure lower than 10^{-5} mbar.

Structural, chemical and morphological results as well as surface data are shown in Table 2.

2.4. Zeolite-modified electrode manufacturing

Electrodes were composed of a mixture of graphite paste (C paste) and zeolite. The C paste was obtained by adding Nujol (paraffin) to graphite in a 30% mass ratio. This makes it possible to have an electric contact due to graphite and a mechanical stability due to the Nujol presence. Zeolite-modified electrodes (called ZME [23]) were obtained by a mixture of 30% of zeolite with the C paste described previously. This ZME (0.22 g) was kept to fill a carbon cup used as electrode support (see below). Care has been taken to keep this mass constant, since in addition to the affinity between the adsorbent and the adsorbate, the amount of *p*-cresol adsorbed directly depends on the amount of zeolite present.
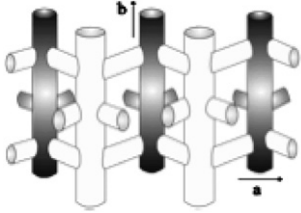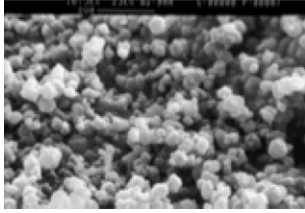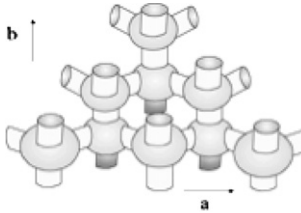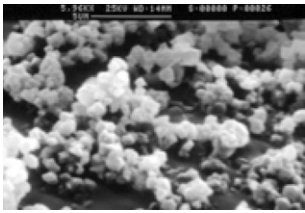
The electrode was constituted by an 8-mm diameter carbon cup filled with the studied zeolite/graphite paste under investigation, as described in the literature [24]. The electrical contact was established using copper wires previously put in a glass tube connected to copper wires using a silver paste. The complete set-up is embedded in an epoxy resin so as to leave only the active part of the electrode exposed to the solution under investigation, as shown in Fig. 1.

2.5. Electrochemical experiments

Electrochemical experiments were performed using PowerSuite software on a PARSTAT 2273 apparatus from Princeton Applied Research. Cyclovoltammetric

Table 2
Resume of structural properties, representation of channel system, scanning electron microscopy images and surface area information determined by nitrogen adsorption at 77 K

Zeolite	Channel system	SEM image	Nitrogen adsorption
MFI with H$^+$ as charge compensating cation, Si/Al ratio 400			BET surf: 273 m^2 g^{-1} Int surf: 209 m^2 g^{-1} Ext surf: 64 m^2 g^{-1}
FAU with H$^+$ as charge compensating cation, Si/Al ratio 160			BET surf: 700 m^2 g^{-1} [a]

BET surf: it is the BET surface; Int Surf and Ext Surf are the internal surface and the external surface, respectively, determined by *t*-plot method.
  [a] The surface area given by the Zeolyst Incorporated.

measurements were carried out at room temperature, with a 10 mV/s scan rate, in a classical three-electrode cell. The saturated calomel electrode (SCE) was used throughout the work, and all the potentials are given with respect to this reference. The counterelectrode was a platinum grid. Oxygen present in the electrolyte solution was driven out using an inflow of argon, while the gas phase in contact also consisted of argon.

The carbon cup was filled with a new ZME mixture for each experimental condition tested. Zeolites used for the manufacturing of ZME were MFI (HMFI and NaMFI H/Na = 50%) and HFAU.
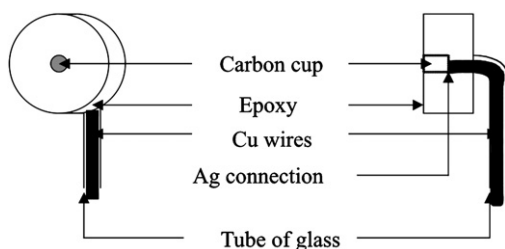

Fig. 1. Scheme of the electrode used as carbon paste electrode when the cup is filled with carbon paste or zeolite-modified electrode (ZME) when the cup is filled by a mixture of carbon paste and zeolite.

For comparison, a simple glassy carbon electrode (0.07 cm^2) and a carbon cup filled with pure carbon paste without zeolite were used. The glassy carbon electrode was polished before the experiment for 15 min using a 6-μm-size diamond paste on polishing clothes.

The electrolyte consisted of either a pure physiological solution (Dubelco Phosphate Buffer Saline (referred as DPBS)) or of a 2 mM *p*-cresol in DBPS. DPBS was purchased from Invitrogen. It contains: NaCl (8 g L^{-1}), CaCl$_2$ (0.1 g L^{-1}), MgCl$_2$ (0.1 g L^{-1}), KCl (0.2 g L^{-1}), KH$_2$PO$_4$ (0.2 g L^{-1}) and NaH$_2$PO$_4$ (2.16 g L^{-1}). Other toxin concentrations were also tested. Water employed was purified by Millipore milliQ filtration system.

During the first experiments, voltammograms were performed directly in the standard *p*-cresol solution to verify the electrochemical oxidation of the toxin. In order to check the influence of the porous volume of the electrode on the electro-oxidation process, experiments were performed under release conditions. For that, we first made an impregnation of the electrodes in the *p*-cresol solution for 12 h. Then, the electrodes were plunged in DPBS where electrochemical experiments were made. Some complementary tests were realized by varying the impregnation time to have a better understanding of the adsorption kinetic of the *p*-cresol in a MFI-type zeolite.

2.6. Independent verification of the quantity of p-cresol adsorbed

With the aim to verify our electrochemical results with respect to classical adsorption measurements, experiments were carried out in batch conditions by depletion method at 37 °C with a liquid/mass ratio equal to 50. The HMFI and HFAU zeolites successively used as adsorbent were put in $C_0 = 9.4$ mM *p*-cresol in physiological solution. Agitation was provided for 12 h, which is a sufficient time to reach equilibrium. Then, liquid and solid were separated by centrifugation at 4000 rounds per minute and the remaining concentration C of *p*-cresol in supernatants was determined using a HPLC set-up (Agilent 1200 series) with a diode array detector and an Agilent Zorbax SB-C18 column using an external standard. The UV measurements were performed at 220 and 277 nm. The amount of *p*-cresol adsorbed (q) was obtained using Eq. (1):

$$q = \frac{(C_0 - C)V}{m} \tag{1}$$

with C_0: initial concentration, C: equilibrium concentration, V: volume of solution and m: mass of solid.

3. Results and discussion

3.1. Electro-oxidation of p-cresol

In a first step, experiments were performed on glassy carbon in order to evidence the potential where electro-oxidation of *p*-cresol occurs. In the literature, several oxidation products are mentioned, such as 3-methyl-1,4-benzoquinone [25]. The hydroxyl group in *para* position of cresol should be oxidized to quinone. The measurement was performed directly, i.e. from 2 mM *p*-cresol in DPBS electrolyte.

Fig. 2 presents the curve obtained on a bulk glassy carbon electrode for the following scan: 0, −0.8, 1.2 V. In the cathodic part no current was observed, indicating no reduction reaction. The solution is properly deaerated because no reduction current due to the presence of oxygen appears. In the anodic region, from 0.5 V, a broad peak corresponding to *p*-cresol oxidation is present ($i_{max} = 100$ μA/cm²). The renewed increase in current observed at about 1.1 V is due to the beginning of water oxidation. During the second cycle performed with the same conditions, no peak was found neither in the anodic nor in the cathodic range, indicating a drastic
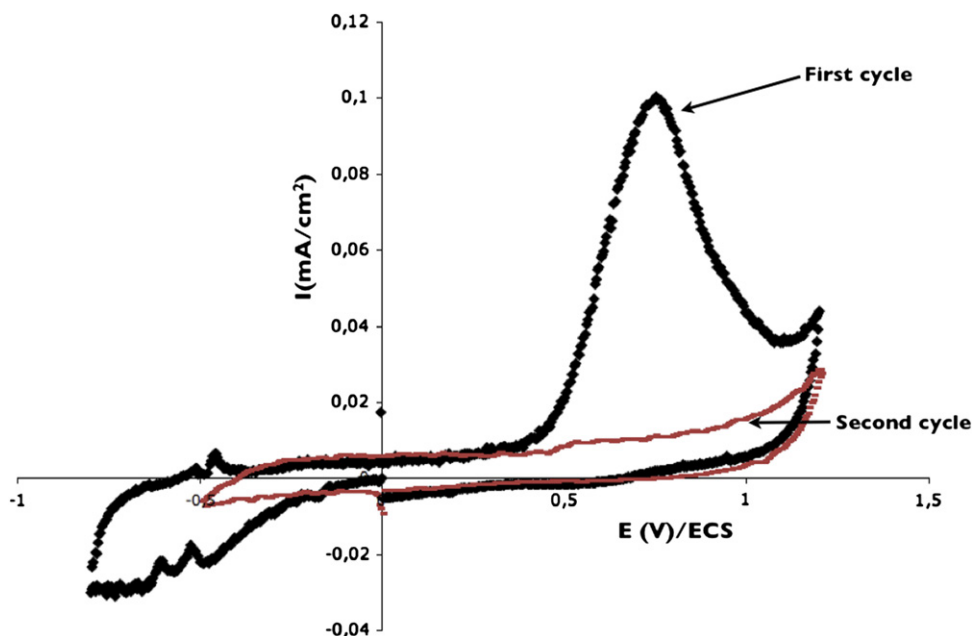

Fig. 2. Voltammograms obtained on bulk glassy carbon electrode in DPBS + 2 mM *p*-cresol solution, using a scan rate of 10 mV/s: first cycle and second cycle.

poisoning of the electrode due to the irreversible *p*-cresol oxidation process. Such a result was already mentioned in the literature on a Pt electrode [26], concerning the fouling of phenolic compounds during the oxidation process [18].

3.2. Results on carbon paste

Fig. 3 shows voltammograms obtained from the carbon paste in 2 mM *p*-cresol + DPBS solution and in pure DPBS, in the absence of zeolite. In both cases, a large current appears on the cathodic part of the curve. It corresponds to the reduction of oxygen that, despite the outgassing of the solution, remains entrapped in the carbon paste. In the anodic part, in DPBS, no peak is observed before the electrolyte oxidation at 1.1 V. From the *p*-cresol-containing solution, two oxidation waves appear, noted Ox1 and Ox2 ($i_{max} = 800\ \mu A/cm^2$), followed by H_2O oxidation. The oxidation current obtained here is about eight times higher than on vitreous carbon, despite the surface normalization. This is due to the larger roughness of the carbon paste that cannot be polished and to possible reactions in the electrode volume because of paste porosity. Note that the second Ox2 peak appears from an equivalent potential than the only peak obtained on vitreous carbon (first cycle in Fig. 2). The registration of successive curves shows a decrease of the two peaks (Ox1 and Ox2), but weaker than on vitreous carbon, evidencing

that the poisoning of the electrode occurs in a less drastic way. Nevertheless, to obtain reproducible experiments, the carbon paste has to be changed for each measurement.

3.3. Zeolite effect: tests on HMFI

Fig. 4 presents the voltammogram obtained on the ZME made by a mixture of HMFI with carbon paste, in a *p*-cresol-containing solution. For comparison, the curve obtained previously on the carbon paste is added. It can be seen that the two oxidation peaks are kept. The influence of the presence of zeolite appears both in the cathodic and anodic parts: the currents due to oxygen reduction and *p*-cresol oxidation are enhanced. In the anodic part, i_{max} obtained in the presence of ZME is three times higher than that on the carbon paste electrode, for an equivalent roughness. This is due to a higher amount of *p*-cresol entrapped in the porous volume of the zeolite. The beneficial effect of the zeolite on the electrochemical oxidation is obvious.

3.4. Experiments during release

Fig. 5 is an overlay of five successive cycles of the electrode obtained in DPBS solution, after an impregnation of the ZME in the 2 mM *p*-cresol electrolyte. These curves are similar to those previously obtained by direct measurement in Fig. 4, the two oxidation
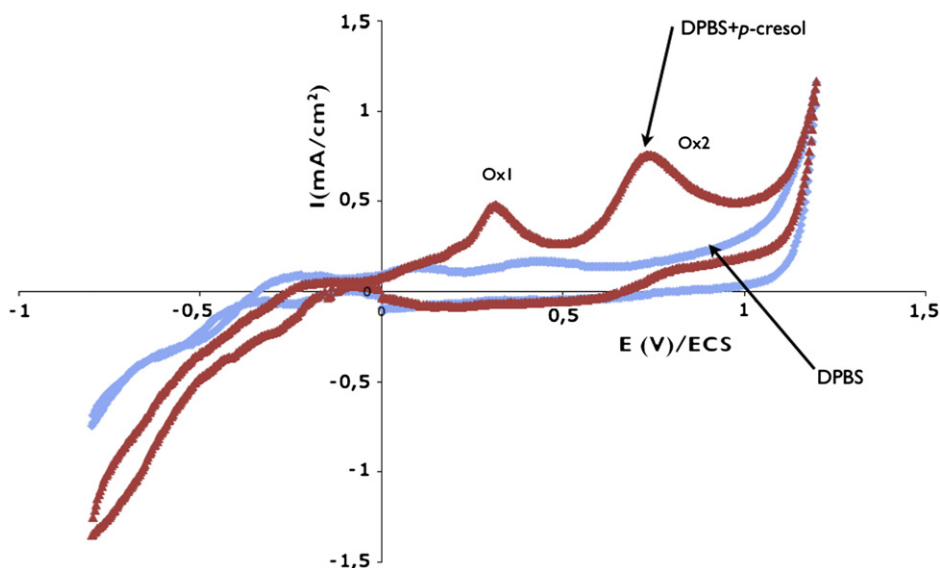

Fig. 3. Voltammograms obtained on carbon paste without zeolite by direct measurement in DPBS and in DPBS + 2 mM *p*-cresol solutions. Scan rate: 10 mV/s.
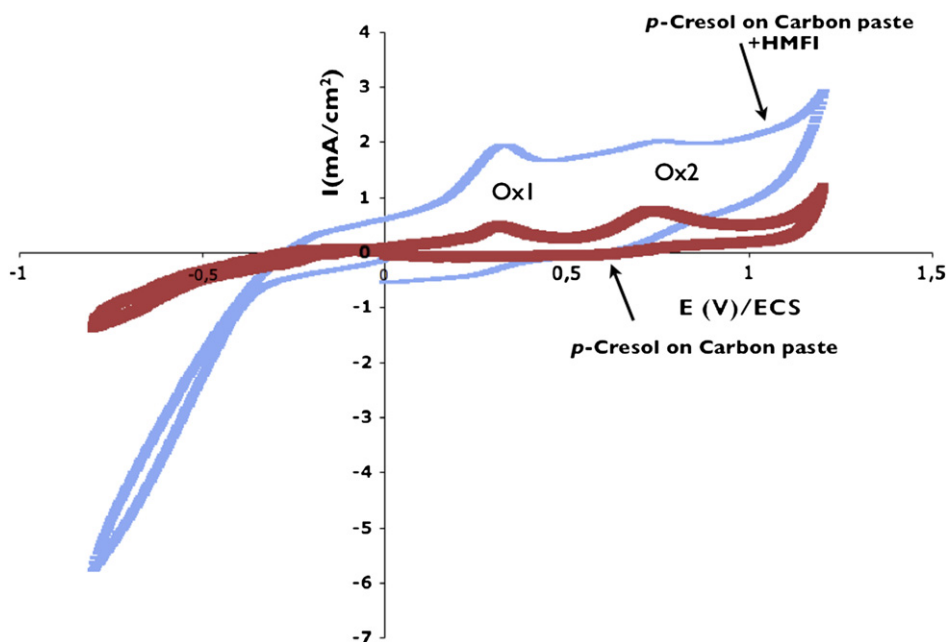
Fig. 4. Evidence of zeolite effect by comparison of voltammograms obtained on carbon paste with and without HMFI zeolite. Measures performed in DPBS + 2 mM *p*-cresol solution. Scan rate: 10 mV/s.

waves remain present. The successive curves performed lead to a decrease in current more important for the first anodic peak than for the second. It can be noted that the poisoning of the ZME is less drastic than on vitreous carbon because there is only a current decrease instead of its complete loss performed on vitreous carbon from the second cycle.

The number of cycles has also an important effect on the cathodic part, due to a decrease of the oxygen quantity entrapped in the microporous volume with cycling.
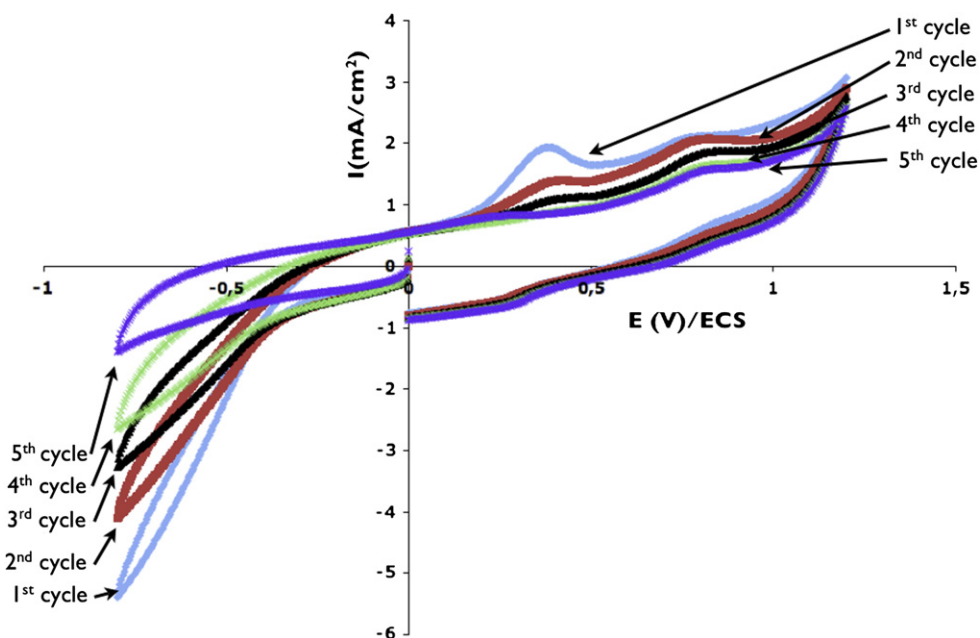

Fig. 5. Influence of the number of cycles performed on the *p*-cresol oxidation waves. Results obtained on HMFI ZME during release (impregnation in a *p*-cresol-containing solution followed by a transfer of the electrode in pure DPBS solution). Scan rate: 10 mV/s.

In order to get a better understanding of the origin of the two oxidation peaks, an experiment is also performed on the carbon paste electrode under release conditions. In that case only one small oxidation peak is obtained $(i_{max} = 0.2$ mA/cm^2) showing the little quantity of p-cresol entrapped in the carbon pore volume of electrode.

Two kinds of oxidation sites are probably present, one in the volume and another on the surface of the ZME.

3.5. p-Cresol concentration measurement (sensor effects)

In order to determine the adsorption isotherm of p-cresol in HMFI, experiments were conducted during release by using different p-cresol concentrations for the impregnation electrolyte. Voltammograms were traced in the same conditions as above and the maximum of the Ox2 peak was noted for each concentration. To check the reproducibility, the measurement at 2 mM concentration was repeated twice. Fig. 6 shows a linear correlation between the maximum current intensity of the Ox2 peak and the concentration of p-cresol in solution. It can be directly related to the quantity adsorbed on the zeolite. The good reproducibility can be seen by the value of the determination coefficient and the exemplary reproducibility shown at the 2 mM p-cresol concentration. Therefore, the conclusion can be drawn that p-cresol concentration in physiological solution can be determined by electrochemical methods. Moreover, the electrolyte/zeolite ratio used in this study is very high (around 3000: 0.22 g of ZME containing
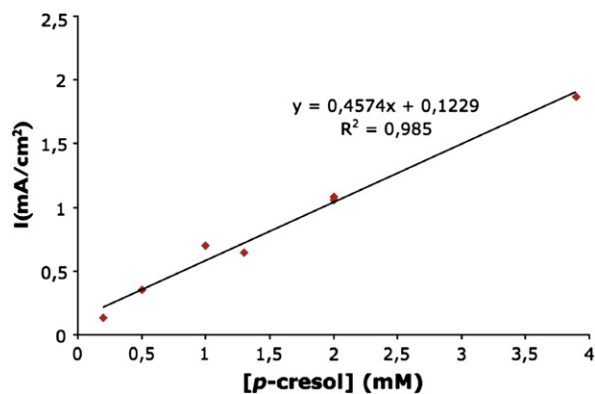

Fig. 6. Variation of the maximum in current for the second oxidation peak as a function of the p-cresol concentration used during the impregnation of HMFI ZME. The corresponding voltammograms were obtained during release, after impregnation in different p-cresol solutions followed by a transfer of the electrode in DPBS. Scan rate: 10 mV/s. The 2 mM point was made twice.

30% of zeolite in 200 ml of solution) in comparison with concentration measurements used in the context of classical isotherm processes, where the ratio is about 50. This high ratio coupled with the high value of the line slope shows that the electrochemical method is sensitive to determine the concentration of p-cresol in solution, even at low concentrations.

3.6. Influence of charge compensating cation

In order to evaluate the influence of zeolites' charge compensating cations on the electrochemical oxidation of alcohol, a sodium form of MFI zeolite was prepared. The parent HMFI zeolite was subjected to an ion exchange using a one molar sodium chloride solution. The electrochemical experiments were made on this ZME by performing a cyclo voltammogram directly in p-cresol electrolyte with various p-cresol concentrations. Here the experiments were not performed in release mode, in order to limit the pure chemical diffusion of Na$^+$ from the zeolite to the solution. The voltammograms obtained on NaMFI are plotted in Fig. 7 for two concentrations of cresol in electrolyte. Those obtained on HMFI are superposed. The presence of Na$^+$ as the charge-compensating cation increases clearly the electrochemical response of p-cresol oxidation, especially at low toxin concentration. This result is in agreement with the literature concerning phenol species. Indeed Carvalho et al. [19] have shown an easier oxidation of phenol in zeolite containing a low level of H$^+$ as charge compensating cations. The oxidation of one alcohol molecule is generating one proton, a high pH promotes this process. This behavior can also be explained by the boundary between the three phases constituted by the carbon paste, the zeolite and the liquid electrolyte. This boundary between the three phases represents the electrochemically active site.

3.7. Adsorption kinetics

In order to determine the lapse of time necessary to reach the equilibrium, kinetic measurements were carried out during the release of p-cresol on NaMFI ZME. Measures on electrode in 2 mM p-cresol solution were performed for several exposition times. Then the ZME was transferred in DPBS solution, in which the cyclovoltammograms were performed. Except for $t_{imp} = 0$ where logically no oxidation peak was observed, the curves always exhibit the two peaks corresponding to the oxidation of p-cresol, with a higher current for the second one. Fig. 8 presents the variation of the integrated value of current measured for the second peak
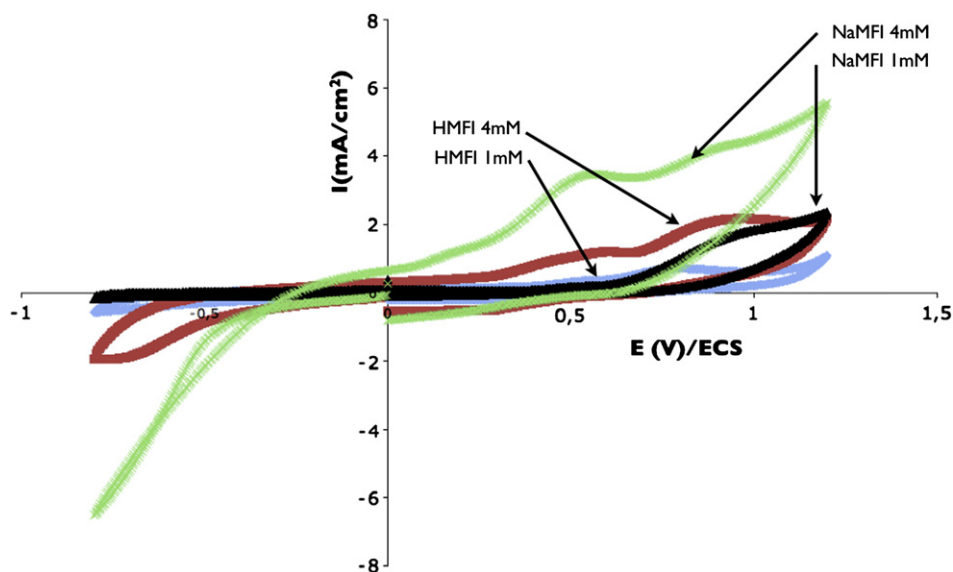
Fig. 7. Evidence of charge compensating cation influence on *p*-cresol oxidation waves. Voltammograms obtained by direct measurement in *p*-cresol + DPBS solution on HMFI and NaMFI ZME. *p*-Cresol concentrations: 4 and 1 mM. Scan rate 10 mV/s.

as a function of the impregnation time. This representation was chosen in order to obtain a better precision. It can be seen that the current value increases almost linearly from 0 to 250 min, then it seems to reach a constant value. This phenomenon is due to the saturation of the zeolite microporous volume by *p*-cresol. Thus, an impregnation time of 250 min seems to be appropriate.

3.8. Zeolite type influence

Generally, the quantity adsorbed by the zeolite depends on the crystallography of the zeolite (network
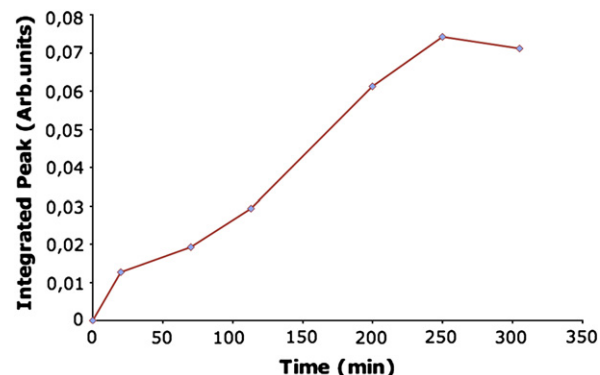

Fig. 8. Influence of the impregnation time of NaMFI electrode on the second oxidation peak obtained on the voltammogram during release in DPBS solution.

structure, pore size) and on its chemical composition. According to the Si/Al ratio, a more or less high number of charge compensation cations will be present in the channels, the zeolite becoming more hydrophobic when the number of cations is small and less acidic when the number of protons is low. Studies have already shown that the adsorption of phenolic compounds in hydrophobic structures is easier for higher Si/Al ratios [19,27].

A new ZME was made using a mixture of FAU and carbon paste in the same proportion than that used above. In that case two opposites parameters are involved: on one side the channel size (pore volume) is increased with FAU ZMEs, but on the other side the Si/Al ratio is decreased (lower hydrophobicity). After an impregnation time of 12 h, for two different *p*-cresol concentrations, cyclovoltammograms were performed in DPBS solution and compared with the corresponding HMFI curves. Fig. 9 shows that the oxidation currents obtained in the case of HFAU are appreciably higher than that in the case of HMFI.

To check this result, complementary adsorption experiments were made in batch condition using depletion method. Adsorption capacities obtained by this method give similar values of 0.36 mmol g^{-1} for HMFI and 0.38 mmol g^{-1} for HFAU, with a difference included in the error range of experiment. From that, it appears that the reduce of affinity caused by the decrease in the Si/Al ratio is compensated by the increase
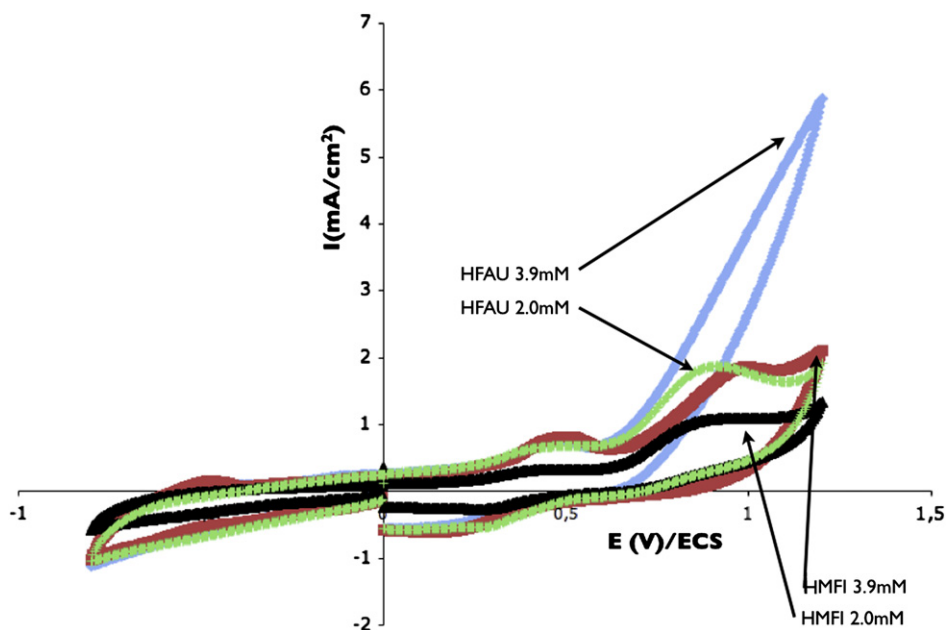
Fig. 9. Influence of zeolite type on voltammograms performed during release in DPBS solution after an impregnation in 2 or 3.9 mM *p*-cresol solution. Electrode used: HFAU and HMFI. Scan rate: 10 mV/s.

of the porous volume. The increase of the oxidation peaks in the case of HFAU ZME obtained in Fig. 9, can then be attributed to an increase of the adsorption reversibility rather than an increase of the amount of *p*-cresol adsorbed in the zeolite.

The properties of adsorption are the limiting conditions for detection by electro-oxidation but the intensity of the current obtained during release is not only related to the adsorption capacity, but also to the adsorption reversibility. The active interface of ZME is constituted by the little interface containing the three phases: carbon paste, zeolite and liquid electrolyte. The electrochemical signal observed is due to the *p*-cresol migration at this interface; the pure chemical diffusion from the zeolite volume to the electrolyte cannot be measured. By comparing two different samples with different adsorbed amounts, the current of oxidation of *p*-cresol for each sample can be different. The current observed is related to the *p*-cresol desorbed at the boundary between the three phases; if the desorption at this interface is higher, the current of oxidation observed is also higher. However, it is very difficult to isolate the influence of one parameter because by changing the zeolite, a lot of structure-type-linked parameters are modified, like surface area, channel system dimensions, organization, pore sizes, hydrophobicity, charge compensating cations and electrochemical interface.

4. Conclusions

The use of a zeolite-modified electrode made of a mixture of carbon paste with MFI or FAU allows us to study the electrochemical conditions for *p*-cresol oxidation. The presence of zeolite in the carbon paste led to an increase of the anodic waves, amplifying the oxidation reaction even at low *p*-cresol concentrations. During the electro-oxidation process, the product of oxidation poisoned the ZME, the fouling of ZME being less important than that on the bulk carbon electrode. On ZME electrodes, two oxidation waves were performed, which corresponded to two kinds of active sites for the *p*-cresol oxidation: surface and new volume sites.

The good adsorption properties of HMFI allow us to determine the *p*-cresol concentration in solution even at low concentration, showing that electrochemical measurements could be used as a detection method with a high sensitivity. In the case of a MFI-type zeolite, the role of charge-compensating cation was studied and shows that the Na^+-containing zeolites presented a more important oxidation capacity for *p*-cresol than in the case of the H^+-containing form. FAU type zeolites, with a larger pore structure but less hydrophobicity than MFI, were also tested. Despite a similar adsorption capacity, the oxidation wave obtained was higher than that with MFI. This behavior could be attributed to

bigger boundaries between the three phases. By changing the type of the nature of the charge-compensating cation or the zeolite type, adsorption properties and especially adsorption capacities could modify the electrochemical behavior. Moreover, substituting a zeolite by another zeolite modifies the active part of ZME, i.e. the boundaries between the three phases. This means that the best adsorbent was not necessarily the best solid for electrochemical detection.

References

[1] P. Brunet, L. Dou, C. Cerini, Y. Berland, Adv. Ren. Replace. Ther. 10 (2004) 310.

[2] G. Lesaffer, R. De Smet, N. Lameire, A. Dhondt, Ph. Duym, R. Vanholder, Nephrol. Dial. Transplant. 15 (2000) 50.

[3] R. Vanholder, R. De Smet, M.A. Waterloos, N. Van Landschoot, P. Vogeleere, E. Hoste, S. Ringoir, Kidney Int. 47 (1995) 510.

[4] L. Dou, E. Bertrand, C. Cerini, V. Faure, J. Sampol, R. Vanholder, Y. Berland, Ph. Brunet, Kidney Int. 65 (2004) 442.

[5] V. Wernert, O. Schaf, H. Ghobarkar, R. Denoyel, Microporous Mesoporous Mater. 83 (2005) 101.

[6] R. Vanholder, R. De Smet, N. Lameire, Contrib. Nephrol. 133 (2001) 42.

[7] D. Berge-Lefranc, C. Vagner, O. Schaf, P. Boulet, H. Pizzala, J.-L. Paillaud, R. Denoyel, Stud. Surf. Sci. Catal. 170 (2007) 1015.

[8] J.P. Peireira Ramos, R. Messina, J. Perichon, J. Electroanal. Chem. 146 (1983) 157.

[9] A. Walcarius, T. Barbaise, J. Bessiere, Anal. Chim. Acta 340 (1997) 61.

[10] H. Ghobarkar, O. Schäf, Y. Massiani, P. Knauth, The Reconstruction of Natural Zeolites, Kluwer Academic Publishers, 2003.

[11] A. Walcarius, Electroanalysis 8 (1996) 971.

[12] A. Walcarius, Anal. Chim. Acta 388 (1999) 79.

[13] B. Liu, R. Hu, J. Deng, Anal. Chem. 69 (1997) 2343.

[14] S. Serban, N. El Murr, Biosens. Bioelectron. 20 (2004) 161.

[15] M.L. Hamlaoui, K. Reybier, M. Marrakchi, N. Jaffrezic-Renault, C. Martelet, A. R.KherratWalcarius, Anal. Chim. Acta 46 (2002) 39.

[16] H. Kotte, B. Grundig, K.D. Vorlop, B. Strehlitz, U. Stottmeister, Anal. Chem. 67 (1995) 65.

[17] M. Xu, W. Horsthemke, M. Schell, Electrochim. Acta 38 (1993) 919.

[18] R.H. Carvalho, F. Lemos, M.A.N.D.A. Lemos, J.M.S. Cabral, F. Ramôa Ribeiro, J. Mol. Catal., A Chem. 248 (2006) 48.

[19] R.H. Carvalho, M.A.N.D.A. Lemos, F. Lemos, J.M.S. Cabral, F. Ramôa Ribeiro, J. Mol. Catal., A Chem. 253 (2006) 170.

[20] V. Wernert, O. Schäf, V. Faure, P. Brunet, L. Dou, Y. Berlan, P. Boulet, B. Kuchta, R. Denoyel, J. Biotechnol. 123 (2006) 164.

[21] W.M. Meier, D.H. Olson, Ch. Baerlocher, Atlas of Zeolite Structure Types fourth revised ed., Elsevier, 1996

[22] H.Y. Van Bekkum, E.M. Flanigen, P.A. Jacobs, J.C. Jansen, Introduction to Zeolite Science and Practice second revised ed., Elsevier, 2001

[23] A. Walcarius, Anal. Chim. Acta 384 (1999) 1.

[24] S. Kilinc Alpat, U. Yuksel, H. Akcay, Electrochem. Commun. 7 (2005) 130.

[25] M.M. Hashemi, B. Eftekhari-Sis, B. Khalili, Z. Karimi-jaberi, J. Braz. Chem. Soc. 16 (5) (2005).

[26] J.-L. Boudenne, O. Cerclier, P. Bianco, J. Electrochem. Soc. 145 (1998) 2763.

[27] D. Bergé-Lefranc, H. Pizzala, J.-L. Paillaud, O. Schäf, C. Vagner, P. Boulet, R. Denoyel, Adsorption 14 (2−3) (2008) 377.